

# Semiconducting behavior of passive film formed on stainless steel in borate buffer solution containing sulfide

Hong-Hua Ge · Xue-Min Xu · Li Zhao ·

Fei Song · Jing Shen · Guo-Ding Zhou

Received: 9 October 2010 / Accepted: 4 February 2011 / Published online: 8 March 2011  
© Springer Science+Business Media B.V. 2011

**Abstract** The semiconducting behavior of passive film formed on 316L stainless steel in borate buffer solution containing sulfide was studied by capacitance measurements (Mott–Schottky approach), electrochemical impedance spectroscopy and potentiodynamic polarization curves. The results reveal that the measured capacitance values of the stainless steel electrode have frequency dependence and hysteresis, which shows amorphous or highly doped semiconductor property of the passive film. The Mott–Schottky plots indicate p-type semiconducting behavior related to chromium oxide and n-type semiconducting behavior to iron oxide at different potential range of stainless steel electrodes. The existence of sulfide in the solution increases the acceptor densities obviously which increase more than five times with the sulfide concentration of 9 mg L<sup>-1</sup> and enables a more conductive behavior. The presence of sulfide also decreases the impedance values and enlarges the passive current of the electrode.

**Keywords** Stainless steel · Passive film · Sulfide · Borate buffer solution · Semiconducting behavior

## 1 Introduction

The anti-corrosion performance of many metals and alloys depends on the protection of the passive film formed on the

surface. The electrochemical behavior of passive film is related to its semi-conductive property in most cases. Hence it is important to know more about the electronic structure of passive film in order to improve the anti-corrosion performance of the materials. However, the major difficulty in studying the electronic structure of passive film on ferritic and austenitic stainless steel is about the complexity of the film formed on Fe–Cr and Fe–Cr–Ni alloys which is composed of different oxides such as chromic oxide, ferric oxide and nickel oxide [1, 2].

Much work has been done to reveal the composition and structure of the passive film formed on stainless steel. Oblonsky et al. [3] found that the passive film on 308 stainless steel consisted of amorphous Fe(OH)<sub>2</sub> and Fe<sub>3</sub>O<sub>4</sub> or γ-Fe<sub>2</sub>O<sub>3</sub>, Ni(OH)<sub>2</sub>, NiO, Cr(OH)<sub>3</sub>, and the Cr(OH)<sub>2</sub>-like species using surface-enhanced Raman spectroscopy. Paola et al. [4] thought that the oxides of iron and chromium coexisted in the passive film on ferritic stainless steel through photoelectrochemical measurement, from which a higher band gap than ferric oxide was obtained and the ferric-chromic oxide solid solution model was proposed according to the photocurrent-potential curves [5]. MacDonald [6] developed the point defect model of passive film, which was based on movement of oxygen and metal vacancy under the action of electrostatic field in the film. The generation of oxygen vacancies on metal/film interface made the barrier layer developed to the metallic matrix and metal vacancies were formed on film/solution interface when metal ions entered into the solution. The passive film exhibited a highly doping structure. According to this model, Latanision [7] proposed that the decrease of oxygen vacancies in Fe–Cr alloy with the increase of the contents of Cr was due to the replacement of vacancies by chromium oxides. The dissolution process of chromium oxides in the passive film was discussed and it was believed that

H.-H. Ge (✉) · X.-M. Xu · L. Zhao ·

F. Song · J. Shen · G.-D. Zhou

Shanghai University of Electric Power, Shanghai Key Laboratory of Colleges and Universities for Corrosion Control in Electric Power System and Applied Electrochemistry, Shanghai Engineering Research Center of Energy-Saving in Heat Exchange Systems, Shanghai 200090, China  
e-mail: gehonghua@shiep.edu.cn

this process led to the formation of duplex structure of passive film, namely the rich-chromium inner layer and poor-chromium outer layer. Bojinov [8, 9] put forward a new model of passive film on Fe–Cr alloys through the measurement of contact resistance, photoelectrochemical method and electrochemical impedance spectroscopy (EIS). He believed that this kind of passive film was composed of one main film and two highly defect interface regions beside it. The main film was similar to an insulator and the two interface regions exhibited n-type and p-type, respectively, according to the type of vacancy/ion and constituting an n-i-p junction in the passive film.

It was shown [10] that the anti-corrosion performance of stainless steel was greatly influenced by sulfide. Many articles focused on the corrosion mechanism of chloride to stainless steel. However, few studies have been reported on the destruction of sulfide. In this study, the measurements of Mott–Schottky plot, EIS, and polarization curve were used to investigate the corrosion mechanism of sulfide to passive film on 316L stainless steel in borate buffer solution.

## 2 Experimental

The working electrodes were prepared from a 316L stainless steel plate with working area of 1 cm<sup>2</sup> and embedded in epoxy resin. The electrodes were polished with different grades of emery papers and then degreased with alcohol and washed with de-ionized water.

Sulfide was added to the borate buffer solution, which was composed of 0.05 mol L<sup>-1</sup> H<sub>3</sub>BO<sub>3</sub> and 0.075 mol L<sup>-1</sup> Na<sub>2</sub>B<sub>4</sub>O<sub>7</sub>·10H<sub>2</sub>O, in the form of Na<sub>2</sub>S·10H<sub>2</sub>O and was newly prepared for each experiment. All experiments were conducted at 45 °C, which is almost the maximum temperature of cooling water in power plant condensers.

All experiments were performed in a three-electrode electrochemical cell with a platinum counter electrode and a saturated calomel reference electrode (SCE). The measurements of Mott–Schottky plot were performed on a CHI660a Electrochemical Workstation at 1000 Hz over a potential range from 0.8 to –1.4 V with a perturbing signal 5 mV. Polarization was applied by successive steps of 50 mV in the cathodic direction. The measurements of the EIS at the open-circuit potential were made by an EG&G PARC M283 potentiostat and a PARC M1025 frequency response analyzer with M398 software over a frequency range from 100 kHz to 0.05 Hz and with ac amplitude 5 mV. The polarization curves were measured at scan rate of 1 mV s<sup>-1</sup> and the working electrode was cathodically treated in the buffer solution at –1.1 V for 5 min before the experiments. All potentials were with respect to SCE.

The fitting of EIS were performed using PAR's 4.51 “Equivalent Circuit” software.

## 3 Results and discussion

### 3.1 Space charge layer capacitance of passive film

#### 3.1.1 Capacitance-potential curve and Mott–Schottky plot of passive film on stainless steel

The passive films of many metals have the properties of semiconductor. When a semiconductor contacts a solution containing redox couples, charges are transferred between the semiconductor and the solution phase. The semiconductor phase and the solution phase will bear opposite charges when static balance is created in the interface. The excess charges in semiconductor phase will distribute in the space charge layer. When the space charge layer is shown as a barrier layer, the relation of the capacitance and the potential obeys Mott–Schottky equation [11]:

$$\frac{1}{C_{sc}^2} = \frac{2}{\varepsilon \varepsilon_0 q N_q} (E - E_{fb} - \frac{kT}{q}) \quad (1)$$

where  $N_q$  represents the donor or acceptor density,  $\varepsilon$  is the relative dielectric constant of the passive film,  $\varepsilon_0$  is the vacuum permittivity,  $q$  is the elementary charge (+e for electrons, and –e for holes),  $k$  is the Boltzmann constant,  $T$  is the absolute temperature, and  $E_{fb}$  is the flat band potential. From Eq. 1, it can be seen that  $C_{sc}^{-2}$  has a linear relationship with potential  $E$ , i.e., the Mott–Schottky plot shows a straight line. For n-type semiconductor, the slope of the straight line is positive. While for p-type semiconductor, the slope is negative. The density of the donor or acceptor  $N_q$  can be derived from the slope of the straight line.

Figure 1 shows the  $C-E$  curve (capacitance and potential relationship) and the Mott–Schottky plot ( $C^{-2}-E$  relationship) of stainless steel electrode in the borax buffer solution. The passive film of stainless steel is composed of the oxides of iron, chromium, nickel, etc., and mainly the oxides of iron and chromium [1–3, 12] as commonly believed. Figure 1 shows a complex capacitance-potential relation where n-type semiconductor behavior appears at higher potential and p-type semiconductor behavior at lower potential. Hakiki [12] believed that when  $E > -0.5$  V, the passive film of stainless steel mainly showed the property of iron oxides and had the structure of n-type semiconductor, but when  $E < -0.5$  V, it showed the property of chromium oxides and had the structure of p-type semiconductor.

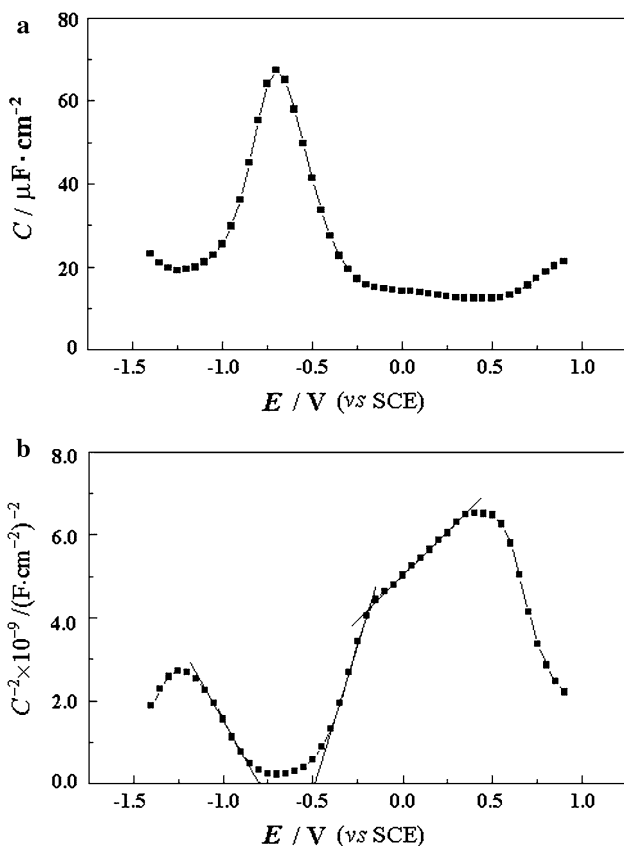


**Fig. 1** The  $C$ - $E$  plot (a) and  $C^{-2}$ - $E$  plot (b) for stainless steel electrode in borate buffer solution

### 3.1.2 The influential factors of capacitance measurement

The  $C$ - $E$  curve measurement is influenced by experiment condition. First of all, different frequencies used directly influence the value of capacitance. Figure 2 shows the  $C$ - $E$  plots (a) and  $C^{-2}$ - $E$  plots (b) for stainless steel measured at different frequencies. The influence of frequency in capacitance measurement is a common phenomenon. Paola [4, 13], and Delnick et al. [14] pointed out that the dependence of capacitance value upon frequency was due to the dispersal of frequency which might be caused by the fringe effect, grain boundary effect of the electrode, slow surface state or slow-response of carriers in the space charge region. The flat band potential can be obtained through the linear fitting of curves in Fig. 2b within the depletion layer in the potential range between -0.5 and -0.2 V. Different flat band potentials were obtained, such as -0.479, -0.475, -0.453, and -0.422 V, at frequencies 1000, 600, 300, and 100 Hz, respectively. The drifting of flat band potential might have something to do with the influence of Helmholtz double layer [15]. If the influence of the surface state is neglected, the experimentally accessible total capacitance  $C$  will consist of the space

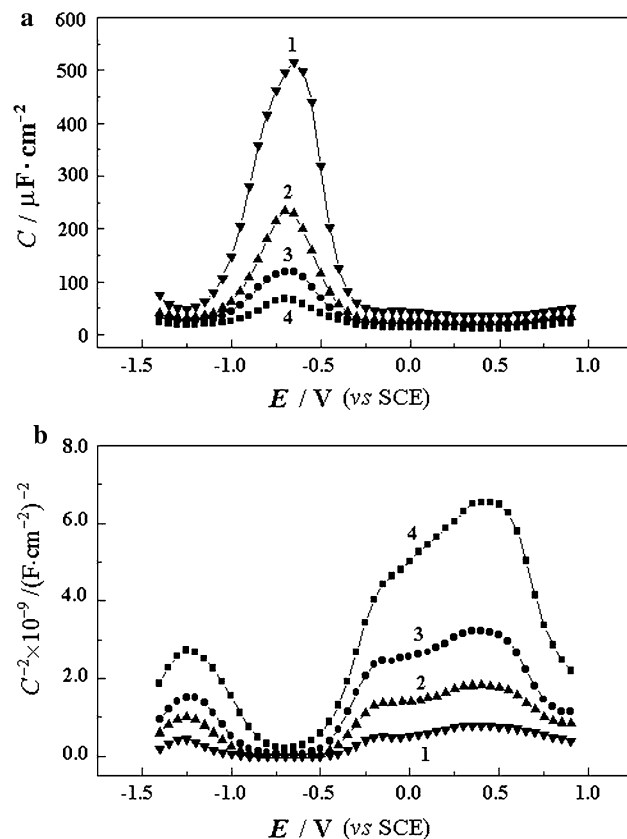


**Fig. 2** The  $C$ - $E$  plots (a) and  $C^{-2}$ - $E$  plots (b) for stainless steel electrodes at different frequencies. Frequency ( $f$ ): (1) 100 Hz; (2) 300 Hz; (3) 600 Hz; (4) 1000 Hz

charge capacitance  $C_{sc}$ , and the Helmholtz capacitance  $C_H$ , in series

$$\frac{1}{C} = \frac{1}{C_H} + \frac{1}{C_{SC}}. \quad (2)$$

As  $C_{sc}$  is much less than  $C_H$  [12], and therefore

$$\frac{1}{C^2} \approx \frac{1}{C_{SC}^2}. \quad (3)$$

As reported in most work, 1 kHz was taken in this article unless otherwise specified.

Different scanning directions in capacitance measurement also make some changes in  $C$ - $E$  curves. Figure 3 is the  $C$ - $E$  curves of scanning to and fro for the stainless steel electrodes within -1.4 to +0.9 V. When potential scan switches from cathodic direction to anodic direction, the changes of capacitance show the hysteresis phenomena. Other researches on carbon steel [16] and 304 stainless steel [5] showed similar results.

Peterson and Parkinson [17] believed that the characteristic of amorphous semiconductor was that there was a high-density of localized state between valence band and conduction band. Dean and Stimming [18, 19] analyzed the

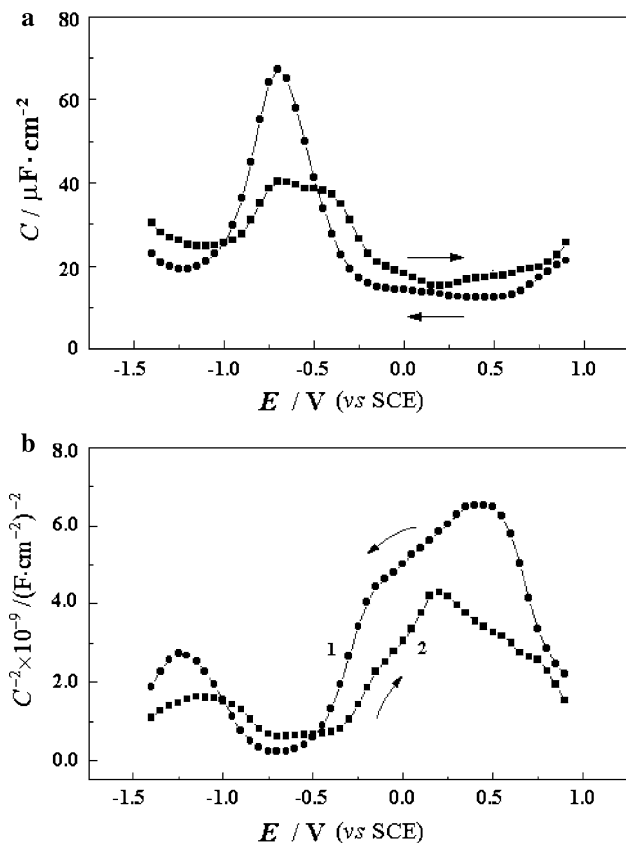


**Fig. 3** The  $C$ – $E$  plots (a) and  $C^{-2}$ – $E$  plots (b) for stainless electrode measured in different scanning directions. (1) in a cathodic direction; (2) in an anodic direction

influence of the localized state in amorphous semiconductor on capacitance and pointed out that the amorphous semiconductor might show Mott–Schottky line, but its capacitance had a larger frequency dependence and hysteresis phenomenon. The hysteresis and frequency dependence of the capacitance of stainless steel electrode in Figs. 2 and 3 indicate that passive film on stainless steel in borax buffer solution is an amorphous or highly doping semiconductor.

### 3.2 Influence of sulfide on the electrochemical behavior of passive film on stainless steel in borax buffer solution

#### 3.2.1 Electrochemical impedance spectroscopy

Figure 4 shows the Nyquist plot of stainless steel electrode in borax buffer solution containing sulfide of different concentrations for 1 h. With the increase of concentration of sulfide, the impedance value of electrode decreases, which indicates that sulfide influences the formation of the anti-corrosion passive film on stainless steel surface.

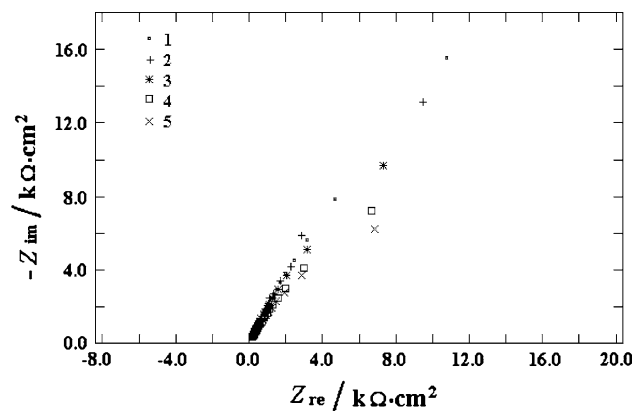


**Fig. 4** The Nyquist plots for stainless steel electrode in borax buffer solution containing various sulfide for 1 h. Sulfide concentration: (1) 0 mg L<sup>-1</sup>; (2) 3 mg L<sup>-1</sup>; (3) 6 mg L<sup>-1</sup>; (4) 9 mg L<sup>-1</sup>; (5) 12 mg L<sup>-1</sup>

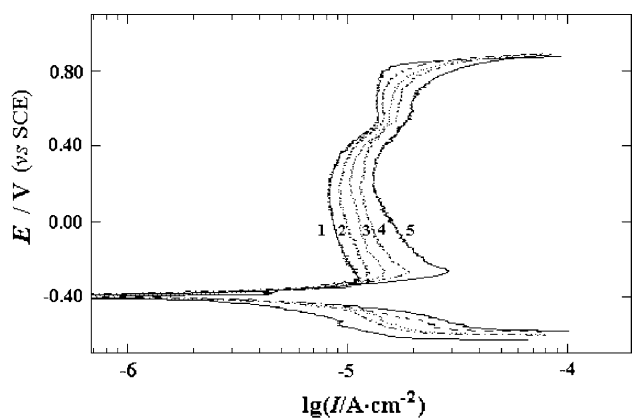


**Fig. 5** The anodic polarization curves for stainless steel electrode in borax buffer solution containing various sulfide. Sulfide concentration: (1) 0 mg L<sup>-1</sup>; (2) 3 mg L<sup>-1</sup>; (3) 6 mg L<sup>-1</sup>; (4) 9 mg L<sup>-1</sup>; (5) 12 mg L<sup>-1</sup>

#### 3.2.2 Anodic polarization curves

Figure 5 is about the anodic polarization curves of stainless steel electrode in borax buffer solution containing sulfide of different concentrations. With increasing sulfide concentration, the passive current density of stainless steel rises, but a change in trans-passive potential is fairly small. Comparison is done using the passive current density  $I_p$  at potential 0 V, as shown in Fig. 6. The results exhibit that  $I_p$  is almost proportional to sulfide concentration. Adding sulfide of 3 mg L<sup>-1</sup> makes  $I_p$  increase from 8.0  $\mu\text{A cm}^{-2}$  to 10.0  $\mu\text{A cm}^{-2}$ , and  $I_p$  increases to 15.3  $\mu\text{A cm}^{-2}$  which is nearly twice as large than that without sulfide when adding sulfide of 12 mg L<sup>-1</sup>.  $I_p$  reflects the dissolution rate of metal through the passive film and its increase shows the decline of protection performance of passive film, indicating that sulfide changes the performance of passive film.

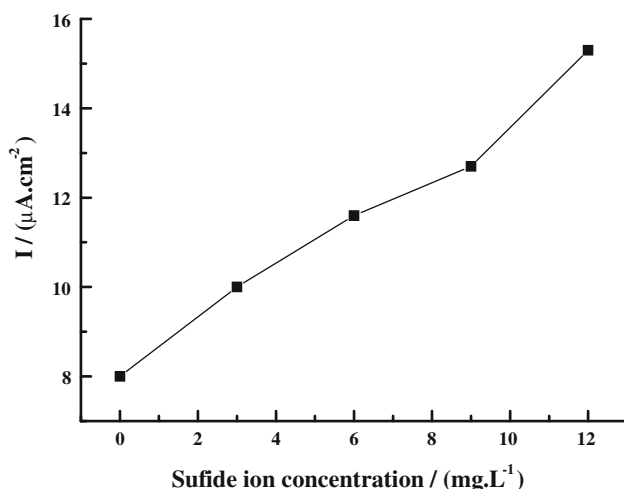


**Fig. 6** The  $I_p$  values at 0 V for stainless steel electrode in borate buffer solution with different sulfide concentrations

### 3.2.3 Influence of sulfide on the semiconductor behavior of passive film on stainless steel

The passive film on stainless steel is mainly composed of iron oxides and chromium oxides. It was suggested by Ferreira after auger analysis, capacitance measurements and photoelectrochemical measurements, that this kind of passive film had a duplex structure. The inner layer was mainly composed of chromium oxides showing the property of p-type semiconductor and the outer layer was mainly composed of iron oxides and hydroxides showing the property of n-type semiconductor [12, 20, 21]. Bojinov et al. [9] studied the anodic film formed on iron–chromium alloy in acid medium and believed that this type of film showed a structure of highly doping n-type semiconductor–insulator–p-type semiconductor. Curve 1 in Fig. 7 is the Mott–Schottky plot for the stainless steel electrode in borax buffer solution in the absence of sulfide after self-passivation for 1 h. It shows four potential regions (I, II, III, and IV) with different capacitance responses. In region I, III, and IV, the passive film shows Mott–Schottky characteristic. The slope of Mott–Schottky plot in region I is negative and shows p-type semiconductor property while in region III, it is positive and shows n-type semiconductor property. Ferreira et al. [12, 20, 21] got similar results for the passive film formed on stainless steel at high temperature and thought that the capacitance response of region I was controlled by chromium oxides in inner layer of the passive film and that of region III was controlled by iron oxides in outer layer of the passive film. Assuming the relative dielectric constant of chromium oxides [22] and iron oxides [23] to be 12, the doping densities of these oxides could be calculated from the slopes of the straight lines in regions I and III, as exhibited in Fig. 8. The donor

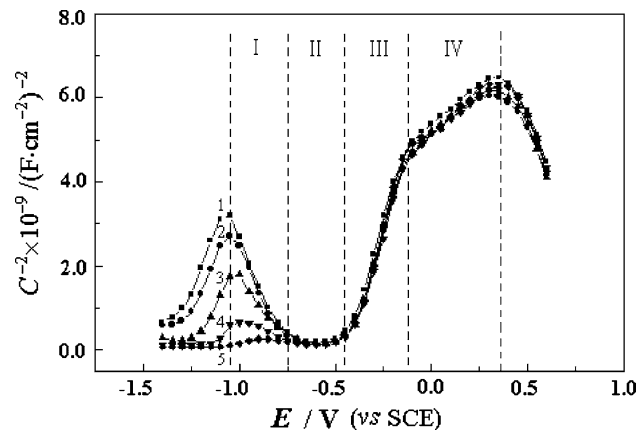


**Fig. 7** The Mott–Schottky plots for stainless steel electrode in borate buffer solution containing sulfide at various concentrations for 1 h. Sulfide concentration: (1) 0 mg L<sup>-1</sup>; (2) 3 mg L<sup>-1</sup>; (3) 6 mg L<sup>-1</sup>; (4) 9 mg L<sup>-1</sup>; (5) 12 mg L<sup>-1</sup>

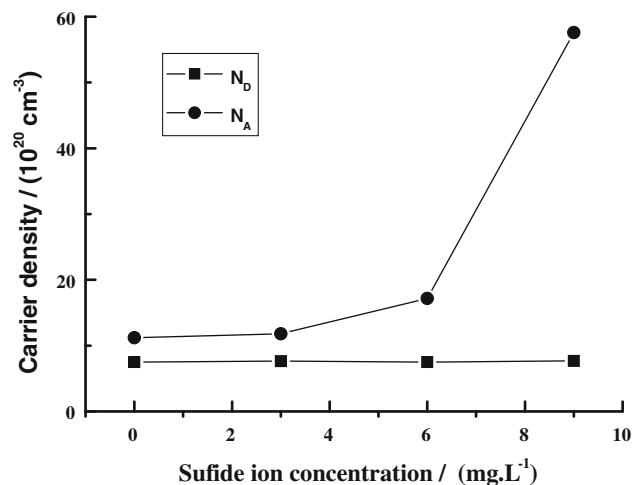


**Fig. 8** The change of donor  $N_D$  (region III) and acceptor  $N_A$  (region I) densities of passive films formed on stainless steel in borate buffer solution with different sulfide concentrations

and acceptor densities of oxides in passive film have an order of  $10^{20}$  cm<sup>-3</sup>, showing a highly doping semiconductor structure. The appearance of region IV is attributed to the existence of second donor level in passive film, which corresponds to the ionization of a deeper donor in passive film [24]. When the potential ranges from -0.47 to -0.1 V, the slope of Mott–Schottky plot is related to the shallow donor and while the potential ranges from -0.1 V to +0.35 V the concentration of carriers increases because of the ionization of the deeper donor and the slope of Mott–Schottky plot decreases. Region II is located near the flat band potential and the high capacitance values shown in this region are related to the Helmholtz layer. When the potential is -0.6 V, the capacitance value reaches  $70 \mu\text{F cm}^{-2}$ , which is in accordance with the capacitance ranges of double layer in other works [25].

The curves 2–5 in Fig. 6 are the Mott–Schottky plots of stainless steel electrode immersed in borax buffer solution containing different sulfide concentrations for 1 h. The donor and acceptor densities calculated according to the slopes of corresponding straight lines in region I and region III are shown in Fig. 8. It is shown from Mott–Schottky plots that the slope of the straight line in region I denoting the property of p-type semiconductor decreases continuously with the increase of sulfide concentration and the acceptor density  $N_A$  increases noticeably, while both the slope of the straight line in region III and the donor density  $N_D$  change slightly. The straight line in region I is corresponding to the chromium oxides in passive film. The change of slope of this straight segment shows the change of the properties of chromium oxides in the passive film. The straight segment in region III reflects the property of iron oxides in passive film and it is less affected by sulfide than that in region I. It is concluded that chromium oxides are more easily affected by sulfide than iron oxides, which might be because the standard Gibbs free energy of formation of chromium sulfide is more negative than that of iron sulfide and the adsorption capacity of chromium to sulfur is better than that of iron [26, 27]. So sulfide impacts chromium oxides first and may change the composition and structure of chromium oxides. The protection performance of passive film on stainless steel is closely related to chromium oxides. Hence, change of the properties of chromium oxides in passive film must affect the corrosion resistance of stainless steel.

In researches on the influence of sulfide about corrosion of steel and copper-nickel alloy in 3.5% NaCl and polluted sea water, Hamdy [28] and Al-Hajji [29] found that the existence of sulfide destroyed the passive state of the film on the surface of metals, declined the corrosion potential of the system and accelerated the corrosion of metals. Marcus et al. studied the influence of adsorptive sulfur on Ni [30], Fe–17Cr–13Ni [31], and Fe–15Cr–10Ni [32] alloys using electrochemical and radiochemical technology, photoelectron spectrometry, and scanning tunnel microscope, and believed that in active dissolution region adsorptive sulfur played a catalytic role in the process of metal dissolution. Namely, the presence of sulfur weakened the bonding force of metallic–metallic bond on metal surface, reduced the activation energy of dissolution reaction of metals and promoted the anodic dissolution process [33]. On the other hand, adsorptive sulfur can prohibit or slow down the formation of passive film. The adsorption of OH on metal surface is the pioneer step of the passivation of metal. Sulfur can take the place of OH and then adsorb on metal surface and inhibit the formation of passive film in the end. The XPS measurement showed that S and OH coexisted on metal surface, supporting this kind of statement [34]. In a word, sulfide ion takes the place of OH and

inhibits the formation of passive film. The doping of sulfide to the passive film makes  $N_D$  increase obviously, decreases the film resistance and makes the anti-corrosion performance of passive film decline. Sulfide might join in the formation process of passive film, inhibit the formation of  $\text{Cr}_2\text{O}_3$  in inner layer and change the structure and performance of passive film.

#### 4 Conclusions

During the capacitance measurement of stainless steel electrode, the results are affected by scanning rates and scanning directions. The capacitance of electrode decreases with the increase of test frequency. The change of capacitance shows the hysteresis phenomenon when the potential scan switches from cathodic to anodic direction. The passive film on stainless steel in borax buffer solution is an amorphous or highly doping semiconductor.

The results of EIS and polarization curves show that existence of sulfide in solution makes the impedance value decrease and passive current density increase. Sulfide inhibits or influences the formation process of passive film.

Mott–Schottky plots show that in different potential ranges, stainless steel has different semiconductor properties in borate buffer solution. When the potential ranges from –1.12 to –0.78 V(region I), the slope of Mott–Schottky plot is negative and shows p-type semiconductor property which is controlled by the electric structure of the inner layer chromium oxides of the passive film. When potential ranges from –0.47 to +0.35 V(regions III and IV), the slope of Mott–Schottky plot is positive and shows n-type semiconductor property which is controlled by the electric structure of the outer layer iron oxides of the passive film. The presence of sulfide makes region I change greatly, the slope of the straight line of region I in Mott–Schottky plot decreases gradually and the acceptor density  $N_A$  increases markedly with the increase of sulfide concentration. The addition of sulfide of 9 mg L<sup>–1</sup> could make  $N_A$  increase of more than five times.

**Acknowledgments** The Project was supported by the Shanghai Committee of Science and Technology, China (Grant No. 08DZ2201400, 09DZ0500400, 10DZ0500300, and 10DZ2210400).

#### References

- Olsson COA, Landolt D (2003) *Electrochim Acta* 48:1093
- Kocijan A, Donik C, Jenko M (2007) *Corros Sci* 49:20838
- Oblonsky LJ, Devine TM (1995) *Corros Sci* 37:17
- Paola AD, Quarto FD, Sunseri C (1986) *Corros Sci* 26:935
- Paola AD, Shukla D, Stimming U (1991) *Electrochim Acta* 36:345
- Macdonald DD (1992) *J Electrochem Soc* 139:3434

7. Kloppers MJ, Bellucci F, Latanision RM (1992) Corrosion 48:229
8. Bojinov M, Kinnunen P, Lundgren K et al (2005) J Electrochem Soc 152:B250
9. Bojinov M, Fabricius G, Kinnunen P et al (2001) J Electroanal Chem 504:29
10. Ge HH, Zhou GD, Wu WQ (2003) Appl Surf Sci 211:321
11. Rangel CM, Silva TM, Cunha MB (2005) Electrochim Acta 50:5076
12. Ferreira MGS, Hakiki NE, Goodlet G et al (2001) Electrochim Acta 46:3767
13. Paola AD (1989) Electrochim Acta 34:203
14. Delnick FM, Hackermann N (1979) J Electrochem Soc 126:732
15. Gryse RD, Gomes WP, Cardon F et al (1975) J Electrochem Soc 122:711
16. Cheng YF, Luo JL (1999) Electrochim Acta 44:2947
17. Peterson MW, Parkinson BA (1986) J Electrochem Soc 133:2538
18. Dean MH, Stimming U (1989) Corros Sci 29:199
19. Dean MH, Stimming U (1989) J Phys Chem 93:8053
20. Montemor MF, Ferreira MGS, Hakiki NE et al (2000) Corros Sci 42:1635
21. Carmezim MJ, Simões AM, Montemor MF et al (2005) Corros Sci 47:581
22. Carmezim MJ, Simões AM, Montemor MF, Da Cunha Belo M (1972) J Electrochim Acta 17:151
23. Dean MH, Stimming U (1987) J Electroanal Chem 228:135
24. Kennedy JH, Frese KW (1978) J Electrochem Soc 125:723
25. Cao CN, Zhang JQ (2002) An introduction to electrochemical impedance spectroscopy. Science Press (Chinese), Beijing
26. Marcus P, Ptotopopoff E (1997) J Electrochem Soc 144:1586
27. Marcus P, Protopopoff E (1990) J Electrochem Soc 137:2709
28. Hamdy AS, Sa'eh AG, Shoeib MA et al (2007) Electrochim Acta 52:7068
29. Al-Hajji JN, Reda MR (1993) Corrosion 49:809
30. Marcus P, Elbiache A, Chadli H (1986) Appl Surf Sci 27:71
31. Elbiache A, Marcus P (1992) Corros Sci 33:261
32. Costa D, Marcus P (1994) In: Marcus P, Baroux B, Keddam M (eds) Proceedings of the European symposium on modifications of passive films, The Institute of Materials (EFC 12), p 17
33. Marcus P (1998) Electrochim Acta 43:109
34. Marcus P, Oudar J, Olefjord I (1980) Mater Sci Eng 42:191